Journal of Zhejiang University-SCIENCE A (Applied Physics & Engineering)
ISSN 1673-565X (Print); ISSN 1862-1775 (Online)
www.jzus.zju.edu.cn; www.springerlink.com
E-mail: jzus@zju.edu.cn

Combustion of nitrate ester plasticized polyether propellants*

Xiao-ting YAN, Zhi-xun XIA, Li-ya HUANG, Xu-dong NA†‡

College of Aerospace Science and Engineering, National University of Defense Technology, Changsha 410073, China

†E-mail: ngvjai@126.com

Received Dec. 27, 2019; Revision accepted Apr. 30, 2020; Crosschecked Oct. 10, 2020

Abstract: Nitrate ester plasticized polyether (NEPE) is a kind of high-energy solid propellant that has both good mechanical properties and high specific impulse. However, its unique composition makes its combustion mechanism different from both double-base propellants and composite propellants. In order to study the combustion mechanism of NEPE propellants, we improved the free radical cracking model of previous research to make it capable of predicting the burning rate of NEPE propellants. To study the combustion characteristics and provide data support for the model, an experimental system was built and four kinds of NEPE propellants with different compositions and grain size distributions were tested. The results show that our modified model can reflect the combustion characteristics of NEPE propellants with an acceptable accuracy. The difference between the model and the experimental data is mainly caused by uncertain environmental factors and the ignorance of interactions between components. Both the experimental data and the results predicted by the model show that increasing the backpressure helps to increase the burning rate of NEPE propellants. Furthermore, the grain size of the oxidizer inside the NEPE propellant has a more severe impact on the burning rate but a lighter impact on the burning rate pressure exponent in comparison with the grain size of aluminum. For aluminum-free NEPE propellants, the reaction in the gas phase is dominant in the combustion process while adding aluminum into the propellant makes the solid phase dominant in the final stage. The combustion of fine aluminum particles near the burning surface generates heat feedback to the burning surface which evidently influences the surface temperature. However, the agglomeration of coarse aluminum particles has little effect on the burning surface temperature.

Key words: Nitrate ester plasticized polyether (NEPE) propellant; Combustion; Free radical model; Burning rate
https://doi.org/10.1631/jzus.A1900668 **CLC number:** V41

1 Introduction

Nitrate ester plasticized polyether (NEPE) represents a significant breakthrough in high-energy solid propellants. It combines advantages of both composite propellants and double-base propellants. This means that it has both high energy and good mechanical properties (Luo and Liu, 2007). NEPE has the highest specific impulse among any solid propellants that have been in application in the world. Its standard theoretical specific impulse could be as high as 2685 N·s/kg while its density could be 1.86 g/cm^3 (Davenas, 1997). Because of the unique combustion performance and combustion mechanism of NEPE propellants, existing combustion models for composite propellants and double-base propellants cannot be applied to simulate the combustion process directly. Therefore, it is necessary to develop and improve a model to simulate the NEPE propellant combustion process on the basis of existing models.

The reactions considered during establishing the combustion model of energetic materials have gradually changed from global reactions to specific elementary reactions. Benreuven et al. (1977) and Benreuven (1980) studied the combustion process of cyclotrimethylenetrinitramine (RDX). They believed that

‡ Corresponding author
* Project supported by the National Natural Science Foundation of China (No. 11572349) and the Natural Science Foundation of Hunan Province (No. 2018JJ3606), China
ORCID: Xiao-ting YAN, https://orcid.org/0000-0002-0752-2392; Xu-dong NA, https://orcid.org/0000-0002-7544-3629

there is a total reaction in the liquid phase, evaporation is the vaporization mechanism on the surface, and there are two total reactions in the gas phase. Ermolin et al. (1987) studied the elementary reactions of ammonium perchlorate (AP) and RDX using mass spectrometry measurements of flames. Based on the prediction model of gunpowder's burning rate, Yang et al. (1997) expressed the burning rate of nitramine propellants as a function of the combustion chamber pressure and the propellant composition. Peng and Liu (1990) proposed a composite flame combustion model of the nitramine/AP propellant. Pang et al. (2003) established a physical model of NEPE propellant combustion based on the combustion model of nitramine and AP-CMDB (compound modified double-base) propellants, combined with the combustion characteristics of NEPE propellants. However, this model failed to consider the influence of the particle size on the propellant combustion process. Zhang and Dai (2007) established a combustion model of NEPE propellants using a genetic algorithm-back propagation (GA-BP) neural network, and then simulated its combustion performance under high pressure. Li et al. (2008a, 2008b, 2009) established the calculation formula of the burning rate and the pressure index of NEPE propellants based on the thermal decomposition characteristics and free radical cracking model of NEPE solid propellant. However, the effect of the content and the particle size on the combustion performance cannot be calculated when both RDX and cyclotetramethylenetetranitramine (HMX) exist. Yetter et al. (1995) and Prasad et al. (1997, 1998) discussed the detailed gas-phase reaction mechanism of nitramine propellant and proposed an eigenvalue method to study the combustion of RDX and HMX propellants. The condensed phase reaction mechanism consists of three steps in which both RDX and HMX thermally decompose through two global channels and the third global step describes the reaction between CH_2O and NO_2 at low temperature. Patidar and Thynell (2017), Khichar et al. (2018, 2019), Patidar et al. (2018, 2019; 2020) studied the decomposition mechanism of RDX and HMX using both experimental and computational methods. Mole fraction profiles of the gaseous decomposition products evolving from the liquid-phase HMX and RDX were obtained using Fourier transform infrared (FTIR) spectroscopy. A quantum mechanics calculation was used to study the pathways of decomposition of HMX and RDX. The detailed reaction mechanism in liquid-phase HMX and RDX was extended.

Fang and Li (2001) studied the effect of AP content and its grain size on the combustion process of NEPE propellants. They found that increasing AP content and using the graded AP can improve the combustion behavior. Li et al. (2001) managed to decrease the burning rate of NEPE propellants by means of adjusting the composition and adding some burning rate inhibitors. Li et al. (2002) worked on the effect of AP on the laser ignition process of NEPE propellants and came to the conclusion that AP plays a more important role in decreasing the ignition delay time than HMX. Wang et al. (2004) researched the combustion characteristics of NEPE propellants and the effect of the composition under high pressure conditions. Wang et al. (2015) studied the ignition and the combustion processes by recording the temperature distribution on the burning surface of NEPE propellants under laser irradiation. Xiang et al. (2016) investigated the effect of the oxygen content in the air on the laser ignition process, the first flame position, and the ignition delay time of NEPE propellants. Pang et al. (2010) researched the thermal decomposition behavior and non-isothermal decomposition reaction kinetics of the propellant containing ammonium dinitramide (ADN). They found that the different components decompose separately in four stages. Sun et al. (2018) conducted the thermal property using TG-DSC-MS-FTIR (thermogravimetry-differential scanning calorimetry-mass spectrometry-Fourier transform infrared). It was found that the NEPE propellant experiences five reaction steps and they are attributed by the evaporation and $O–NO_2$ bond breaking of nitrate, crystal transition of HMX, and thermal decomposition of plasticizer, HMX, and AP.

In this paper, we propose a combustion model of NEPE propellants based on the free radical cracking model, and study the effects of grain size, grain size distribution, and the contents of AP, HMX, and Al on the burning rate of NEPE propellants under different pressure conditions. The results calculated by this model are compared with the experimental data, in which four kinds of NEPE propellants with different formulations are tested. The combustion model and the experimental setup are introduced, respectively. The effects of the composition formula, grain size,

and backpressure on burning rate, pressure exponent, and flame structure are analyzed based on the experimental data. Furthermore, the main reason for the difference between the experimental result and the simulation result is discussed. The experimental results validate the accuracy of the combustion model. This means that the proposed model can be a useful tool in studying the combustion mechanism of NEPE propellants.

2 Free radical cracking model

2.1 Burning rate formula

Based on the theory of free radical cracking proposed in (Fry et al., 2002), the burning rate of NEPE propellants was predicted combining the thermal decomposition reaction hypothesis in the initial stage of combustion. The free radical cracking model is a chemical-mathematical model based on quasi-1D gas phase reaction flow combining with mass transfer. This model mainly focuses on analyzing the relationship between the chemical structure and the characteristic reaction (Song, 1986; Wang, 2007). This model uses functions of pressure and parameters related to the decomposition of propellants to calculate the burning rate. This can relatively reduce the difficulty since the calculation of some parameters, such as thermal conductivity, latent heat of evaporation, and reaction activation energy, can be avoided.

This model divides the gas phase decomposition products in the vicinity of the combustion surface during the combustion of solid propellant into five groups, including oxidant [NO_2], reducing agent [CH_2O], cleavable free radical [CHO], neutral group [CH], and neutral group [CO]. The burning rate of propellant is related to the content of these five groups. This model can be used to estimate the burning rate of the propellant since the gas phase decomposition products on the combustion surface are among these five groups of products.

Considering the influence of the particle size and content of each component on the combustion process, the impact factors of each component, f_{Al}, f_{HMX}, f_{AP} are introduced into the formula to calculate the burning rate. The obtained formula is given as follows:

$$u(p)=\frac{1.709p\theta_0^2(p)}{\rho_{\mathrm{P}}}\cdot f_{\mathrm{Al}}\cdot f_{\mathrm{HMX}}\cdot f_{\mathrm{AP}}, \tag{1}$$

where ρ_{P} is the density of NEPE propellant, g/cm^3. p is the pressure in the combustion chamber, MPa. $\theta_0(p)$ is the mole fraction of the oxidizing gas on the burning surface and it is obtained as follows:

$$\theta_0(p)=\frac{1+\alpha_{\mathrm{H}}\cdot\xi(p)}{\alpha+\beta+q\cdot\eta(p)+\gamma+1}, \tag{2}$$

where α, β, q, γ, and α_{H} are respectively the mole ratios of the amount of [CO], [CH], [CHO], [CH_2O], and [N_2O] gas to that of [NO_2] gas of the decomposition products of 1 kg propellant on the burning surface with the surface area δ, and $\alpha_{\mathrm{H}}=a_{\mathrm{HMX}}/\delta$. $\eta(p)$ is a function describing the degree of cracking of [CHO] free radicals as follows:

$$\eta(p)=2-\exp[0.6931(1-p/p^*)\cdot g_{\mathrm{AP}}\cdot g_{\mathrm{Al}}]. \tag{3}$$

$\xi(p)$ is the conversion function of C-N bond cleavage to N-N bond cleavage during the thermal decomposition of nitramine and it is calculated by

$$\xi(p)=\left(1-\mathrm{e}^{-\frac{p}{p^{**}}}\cdot g_{\mathrm{H}}\right)\cdot a_{\mathrm{HMX}}, \tag{4}$$

where g_{H}, g_{AP}, and g_{Al} are coefficients respectively related to the content and grain size of HMX, AP, and aluminum. p^* is the characteristic pressure, namely, 9.81 MPa. p^{**} is the second characteristic pressure whose value is 40.0 MPa. There are several parameters to be determined during the calculation of f_{Al}, f_{HMX}, f_{AP}, g_{H}, g_{AP}, and g_{Al}. Li et al. (2009) suggested that f_{Al}, f_{HMX}, f_{AP}, g_{H}, g_{AP}, and g_{Al} can be obtained using the equations below after analyzing the experimental data. The detailed explanation of this model is listed in Appendix A.

$$g_{\mathrm{AP}}=\left(1+46.26\times\sum_{i=1}^{n}\frac{a_{\mathrm{AP}i}}{d_{\mathrm{AP}i}}\right)^{0.32}, \tag{5}$$

$$f_{\mathrm{AP}}=\left(1+46.26\times\sum_{i=1}^{n}\frac{a_{\mathrm{AP}i}}{d_{\mathrm{AP}i}}\right)\sqrt{1+4\times\left(\sum_{i=1}^{n}a_{\mathrm{AP}i}\right)^2}, \tag{6}$$

$$f_{\mathrm{HMX}}=\prod_{i=1}^{n}\left[1+11.73\times\left(a_{\mathrm{HMX}i}\right)^{\frac{1}{3}}d_{\mathrm{HMX}i}\times10^{-4}\right], \quad (7)$$

$$g_{\mathrm{H}}=f_{\mathrm{HMX}}^{1.2}, \quad (8)$$

$$f_{\mathrm{Al}}=\left(1+0.015\times\frac{a_{\mathrm{Al}}}{d_{\mathrm{Al}}}\right)\sqrt{1+13a_{\mathrm{Al}}}\,\mathrm{e}^{-50(0.1-a_{\mathrm{Al}})^2}, \quad (9)$$

$$g_{\mathrm{Al}}=\frac{1+10a_{\mathrm{Al}}}{d_{\mathrm{Al}}+0.7}, \quad (10)$$

where a is the mass fraction, d is the grain size, and n means the grain size distribution.

2.2 Thermal decomposition law of AP

Wang (2007) showed that the AP undergoes physical and chemical changes at the same time during its combustion process. The total reaction can be approximated as follows:

$$\mathrm{NH_4ClO_4}\rightarrow\mathrm{NH_3+HClO_3+O}. \quad (11)$$

The decomposition products are all in gas phase, where O can be classified as [NO_2], NH_3 can be classified as [CH_2O], and $HClO_3$ can be classified as [CHO]. According to this, the chemical structural parameters can be obtained as α=0, β=0, q=8.51, γ=8.51, and δ=8.51.

2.3 Thermal decomposition law of HMX

According to Palopoli and Brill (1991), the thermal decomposition reaction of HMX can finally be expressed as follows:

$$\mathrm{C_4H_8O_8N_8\ (HMX)}\rightarrow\mathrm{NO_2+HCN+H+3N_2O+3CH_2O}. \quad (12)$$

Among them, NO_2 and N_2O can be attributed to the [NO_2] group, CH_2O can be attributed to the [CH_2O] group, HCN can be attributed to the [CHO] group, and H can be attributed to the [CO] group. According to this, the chemical structure parameters of HMX can be obtained as α=3.38, β=0, q=3.38, γ=10.14, and δ=13.52.

2.4 Chemical structure parameter

Based on the basic method of propellant burning rate prediction, combining the analysis of the thermal decomposition characteristics of the main components in NEPE propellants with the burning rate prediction model of NEPE propellants, the chemical structure parameters of the main components can be obtained, as shown in Table 1.

3 Experimental method

3.1 Experimental scheme

An overall diagram of the experimental apparatus is shown in Fig. 1. The system consists of a vacuum chamber, a resistance wire ignition system, a gas supply system, a control and measuring system, and a high-speed photography system. All combustion tests were conducted in a vacuum chamber under nitrogen atmosphere. The test sample was fixed on the tungsten-rhenium thermocouple with its top near the resistance wire. The pressure in the vacuum chamber and the temperature of the test sample were measured and recorded during the whole experiment. The combustion process was observed and recorded by a high-speed camera. The frame rate of the high-speed camera was set to be 1000 frame/s. The time of exposure was 50 μs for aluminum-free NEPE propellants and 10 μs for aluminum-containing NEPE propellants, since the flame of the aluminum-containing NEPE propellants might be brighter because of the combustion of aluminum.

3.2 Propellant formulations

Fig. 2 shows four kinds of NEPE propellants that were used in the experiment. The test samples in this experiment are typically 5 mm×5 mm×7 mm rectangular bars. To capture the end burning, we used polyvinyl butyral (PVB) in absolute ethyl alcohol as fire retardant. Consequently, the experimental phenomenon would be clearer. Table 2 shows ingredients and weight mixture ratios of the four kinds of test samples. The grain sizes of AP-1, AP-2, HMX-1, HMX-2, Al-1, and Al-2 are 130 μm, 13 μm, 86 μm, 12 μm, 28 μm, and 3 μm, respectively. All samples contain two kinds of oxidizer, AP and HMX. Only KD-3 and KD-4 contain aluminum. KD-1 and KD-2 have the same weight percentage of AP, HMX, and binder. KD-1 has bimodal AP distribution while KD-2 has bimodal HMX distribution. Similarly, KD-3 and KD-4 have the same weight percentages of

AP, HMX, aluminum, and binder, while KD-3 has bimodal AP distribution as well as bimodal HMX distribution and KD-4 has bimodal aluminum distribution. The binder is made of polyethylene glycol (PEG) (25%) and plasticizer (75%), while the plasticizer is composed of nitroglycerin (NG) (50%) and butanetriol trinitrate (BTTN) (50%).

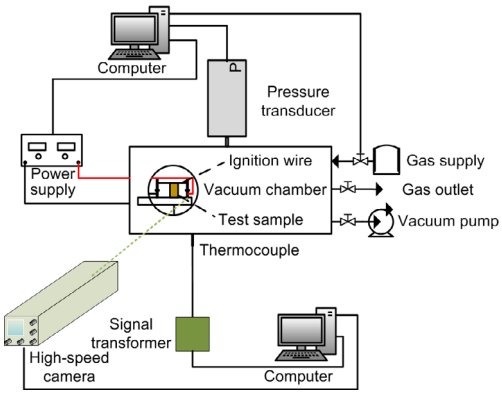

Fig. 1 Overall diagram of the experimental set-up

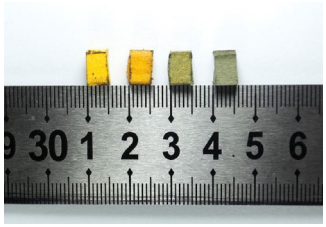

Fig. 2 Four NEPE propellant samples adopted in the experiment

4 Results

4.1 Effect of pressure on the combustion process

Tests were conducted under five different pressure conditions for all four kinds of propellants. Fig. 3 shows the burning rate as a function of the chamber pressure for each sample. It can be seen that when the pressure increases, the burning rates of the aluminum-free NEPE propellants increase rapidly but the increase rates slow down gradually when the pressure is higher than 1.5 MPa. For the aluminum-containing NEPE propellants, the burning rates increase with the chamber pressure and the tendencies are almost linear. This may be caused by the pressure not being high enough. The slope of the ln$p$-ln$r$ curve, which is defined to be the burning rate-pressure exponent according to the Vielle Equation, shows the same trend as that in Fig. 3. KD-2 and KD-3 are relatively more sensitive to pressure.

Fig. 4 shows the flame of the samples at the same reaction stage under different backpressure conditions. We can find that for aluminum-free propellants, as the backpressure increases, the gas-phase flames become brighter and more homogeneous, the diffusion flames are more obvious, and the combustion characteristics of AP composite propellants are more obvious. For aluminum-containing propellants, when the pressure increases, the reaction speeds increase, the release of heat in the reaction zone is more severe, and the flames are also more homogeneous and brighter.

Table 1 Chemical structure parameters of main components in NEPE propellants

Component	Chemical structure parameter					Characteristic pressure (MPa)
	α	β	q	γ	δ	
AP	0	0	8.51	8.51	8.51	9.81
HMX	3.38	0	3.38	10.14	13.52	9.81
NG	0	0	4.405	8.81	13.216	9.81
BTTN	0	0	4.15	8.30	12.45	9.81

Table 2 Ingredients and weight mixture ratios of tested NEPE propellants

Propellant sample	Weight mixture ratio (%)						
	AP-1	AP-2	HMX-1	HMX-2	Al-1	Al-2	Binder
KD-1	10	10	48	–	–	–	32
KD-2	20	–	24	24	–	–	32
KD-3	8	8	20	20	18	–	26
KD-4	16	–	40	–	9	9	26

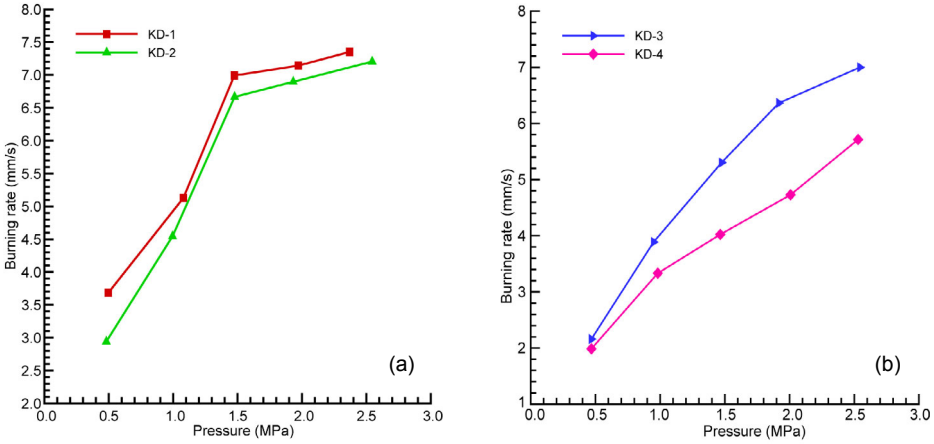

Fig. 3 Burning rate as a function of the environmental pressure
(a) Aluminum-free NEPE propellants; (b) Aluminum-containing NEPE propellants

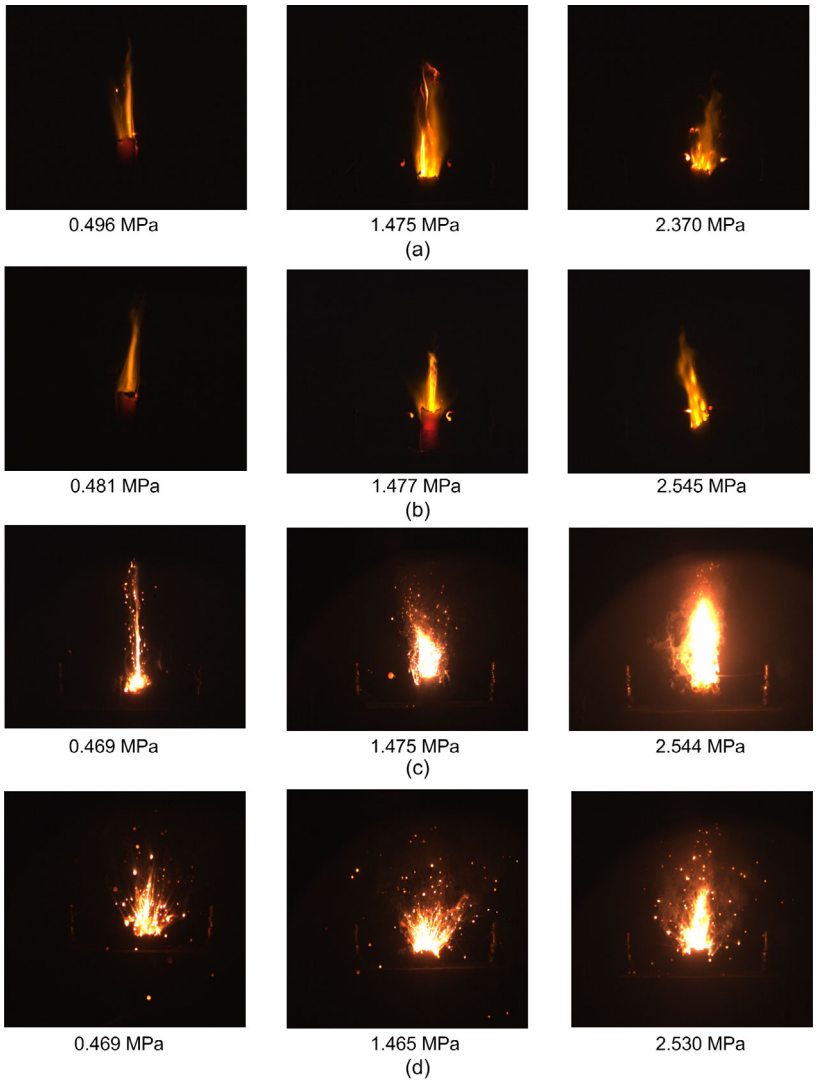

Fig. 4 Flames of NEPE propellants at the same reaction stage but different backpressure conditions
(a) KD-1; (b) KD-2; (c) KD-3; (d) KD-4

4.2 Effect of composition formulation and grain size distribution on combustion

Fig. 3a shows that for aluminum-free NEPE, the burning rate of KD-1 is always higher than that of KD-2 under the same backpressure. According to Table 2, KD-1 and KD-2 have the same ingredients but different grain size distributions. KD-1 contains AP of smaller grain size while KD-2 contains HMX of smaller grain size. It is known that the decrease of grain sizes of both AP and HMX would cause the increase of the burning rate (Liu et al., 2003). As a result, the grain size of AP has more impact on both the burning rate and the burning rate pressure exponent of NEPE propellants than that of HMX for aluminum-free NEPE propellant.

As for aluminum-containing NEPE propellant, the burning rate of KD-3 is always higher than that of KD-4 under the same backpressure (Fig. 3b). Similarly, it can be found from Table 2 that KD-3 and KD-4 have the same ingredients, but different grain sizes. KD-3 contains AP and HMX with smaller grain sizes while the grain size of aluminum in KD-4 is smaller than that in KD-3. The decrease of grain size of aluminum causes the increase of burning rate. It indicates that the grain size of the oxidizer has more impact on the burning rate but less impact on the burning rate pressure exponent than that of aluminum for aluminum-containing NEPE propellant.

Fig. 5 shows the flames of KD-1 and KD-2 in the initial and final stages of the combustion process when the backpressure is 2 MPa. The flame structures are basically the same for all diffusion flames in the initial stage and premixed flames in the final stage, suggesting that neither the grain size of AP nor the grain size of HMX has much impact on the flame characteristic. In the initial stage, the flame of KD-1 is smaller than that of KD-2, while the characteristic of the premixed flame is more obvious for KD-2 because the flame is thinner and longer. The reason is that AP particles with smaller grain size in KD-1 would gasify, decompose, and then combust near the burning surface more quickly. Then the flame becomes closer to the burning surface. KD-2 contains HMX with smaller grain size, which causes the faster formation of molten blends in the molten layer and the faster transformation from diffusion flame to premixed flame. Combining it with burning rates of KD-1 and KD-2, we can conclude that the decomposition of AP has more impact on the combustion process than the molten blends in the final stage of combustion, which means that it is the gas-phase reaction zone that dominates the combustion process.

Fig. 6 shows the flames of KD-3 and KD-4 in the initial and final stages of the combustion process under the backpressure of 0.469 MPa. In the initial stage of combustion, there are more aluminum particles escaping from the surface of KD-4. Moreover, a broader distribution of aluminum particles is found in the gas phase for KD-4. In the final stage, the

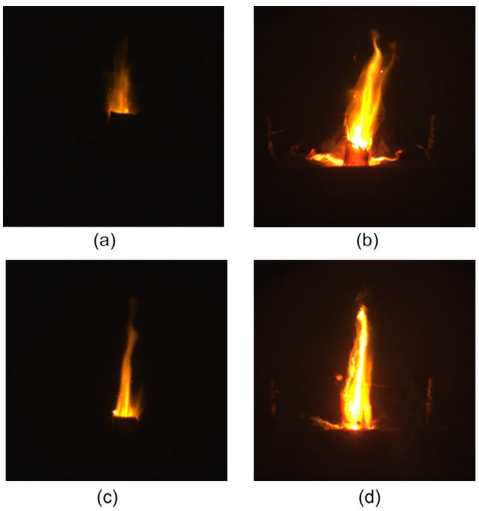

Fig. 5 Flame characteristics of KD-1 and KD-2 under 2 MPa backpressure condition

Initial stage (a) and final stage (b) of combustion for KD-1; Initial stage (c) and final stage (d) of combustion for KD-2

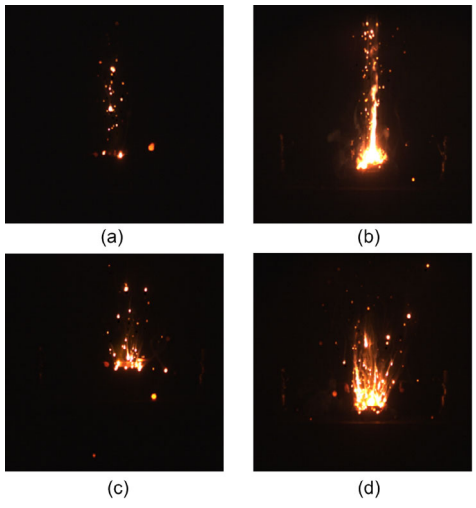

Fig. 6 Flame characteristics of KD-3 and KD-4 under 0.469 MPa backpressure condition

Initial stage (a) and final stage (b) of combustion for KD-3; Initial stage (c) and final stage (d) of combustion for KD-4

flame of KD-3 is thinner and longer with more characteristics of the premixed flame. It means that in the first stage, aluminum particles with smaller grain size in KD-4 more easily escape from the surface under the effect of gas flow and have a broader range for movement. Furthermore, aluminum particles with smaller grain size are more easily ignited, which makes the flame of KD-4 brighter than that of KD-3. In the final stage of the combustion process, the molten blends of nitramine and energetic binder gradually become dominant. KD-3 has a more obvious premixed flame than KD-4 because KD-3 contains HMX with smaller grain size, which more easily decomposes. Combining this phenomenon with the burning rates of KD-3 and KD-4, we can conclude that the molten blends in the final stage have more impact on the combustion process. That is why the grain size of aluminum has more impact on the ignition delay time but less impact on the burning rate than does the grain size of oxidizers.

Since the error of backpressure is less than 5%, it can be considered that Table 3 shows the temperature on the burning surface of four kinds of NEPE propellant samples under approximately the same backpressure. After the addition of aluminum particles with small grain size, the burning surface temperature clearly increases. It is already clear that the aluminum particles will undergo endothermic physical changes such as preheating, oxide film rupture, and melting on the combustion surface and the sub-combustion surface. However, the temperature increase and the flame structure reflect that additional heat may be transferred to the combustion surface, causing the temperature of the combustion surface to rise. This additional heat is generated by the primary combustion of some aluminum particles on the combustion surface and the ignition and combustion process of other aluminum particles in the gas phase zone close to the combustion surface. Decreasing the grain size of aluminum has more impact on the burning surface temperature than the oxidizer. This suggests that there is significance in the heat feedback of aluminum particle combustion to the heat balance of the burning surface.

Table 3 Temperatures on the burning surface under approximate backpressure condition

NEPE propellant	Pressure (MPa)	Burning surface temperature (°C)
KD-1	0.496	380
KD-2	0.481	478
KD-3	0.469	456
KD-4	0.469	692

4.3 Comparison between simulation and experimental results

Based on the free radical cracking model, we developed and improved a code to predict the burning rate of NEPE propellants. The simulation results are compared with the experimental results to verify the rationality and accuracy of the model. Figs. 7a–7d show the results of four kinds of NEPE propellants under different pressures.

Figs. 7a–7d show that as the pressure increases, the burning rates of all the four kinds of propellants increase. The burning rate of KD-2 is always lower than that of KD-1 and the burning rate of KD-4 is always lower than that of KD-3. This is consistent with the burning rate trends in the combustion experiment. It means that simulation results obey the variation law of the burning rate as a function of pressure. In addition, the effect of the composition and grain size of each component on the burning rate is also reflected. Therefore, this model can be used to predict the variation law of the burning rate and can provide, to some extent, qualitative guidance for the composition design of NEPE propellants.

Although the simulation results show the same trend and variation law as experiment, it is clear that the difference between them is relatively large, which is mainly caused by the incompleteness and idealization of this model. The weakness of this model is that the interaction between AP and HMX is not considered, while regarding AP and HMX as being thermally decomposed separately. In the actual reaction process, AP and HMX have a “chain interaction” mechanism (Li and Fang, 2002), which not only causes effects on each other at the initial stage of ignition, but also causes the transfer of exothermic process and reactions between decomposition products in the subsequent combustion process. Ignoring this process can have a great impact on the burning rate simulation results.

According to Figs. 7a–7d, the error between the simulation value and the test value of KD-2 and KD-3 is significantly larger than that of KD-1 and KD-4. Both KD-2 and KD-3 contain two kinds of HMX of different sizes, which indicates that the effect of

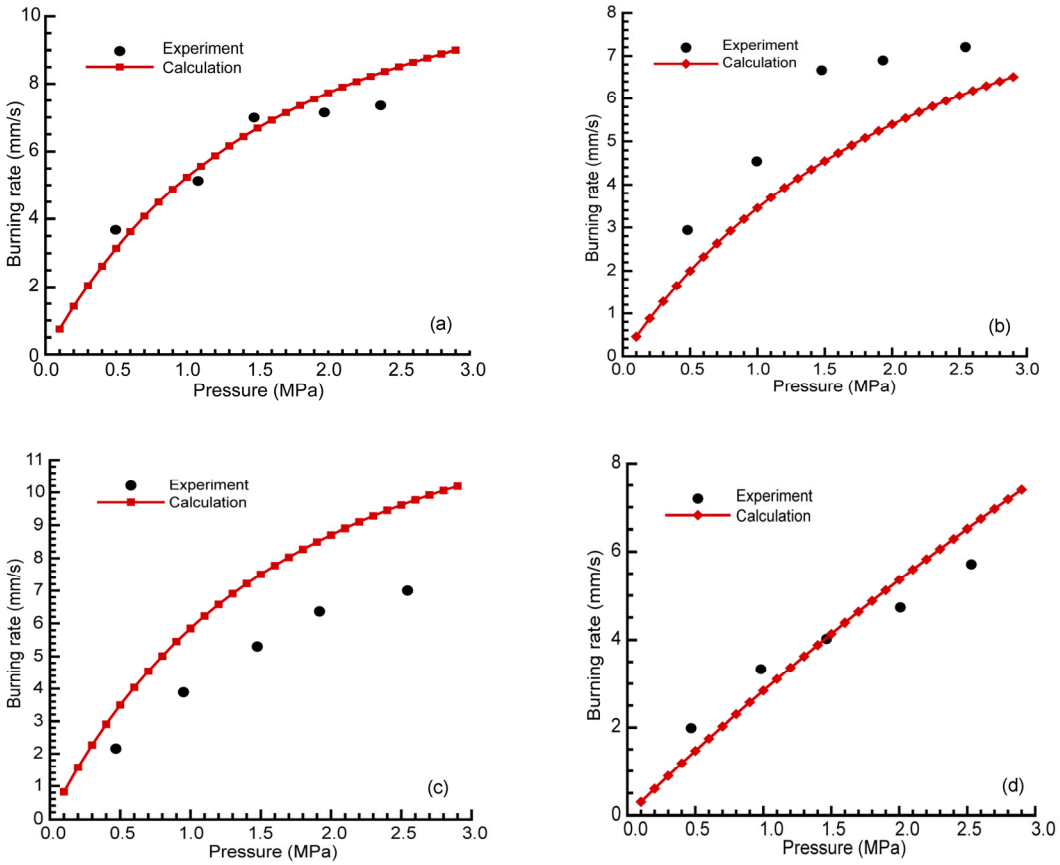

Fig. 7 Comparisons of experimental results and simulation of KD-1 (a), KD-2 (b), KD-3 (c), and KD-4 (d)

HMX on the combustion process is not fully considered in the model. During the combustion process of NEPE propellants, the thermal decomposition of HMX not only affects the combustion process in the gas phase reaction zone, but also plays an important role in the molten layer. The effect of HMX, especially those with the smaller grain sizes, on the combustion process should attract attention since HMX with smaller grain sizes decomposes more quickly and causes greater impact. The interaction of HMX of different grain sizes should also be considered in the model.

Experimental study showed that the burning rate of KD-3 is always lower than that of KD-2 under the given pressure range. According to the burning rate data provided by the propellant producer (Hubei Institute of Aerospace Chemical Technology, China), the burning rate of KD-3 turns out to be higher than that of KD-2 only after the pressure is higher than 3 MPa. However, the simulation results show that the burning rate of KD-3 is always higher than that of KD-2, which is inconsistent with common sense, indicating that the effect of aluminum particles, especially aluminum particles with larger grain size on the combustion process under low pressure was not fully considered. In the actual combustion process, aluminum particles undergo endothermal physical changes including preheating, oxide film rupture and melting, and exothermal chemical change including combustion. Furthermore, the grain size of aluminum particles and the external pressure do affect the escape of aluminum particles from the surface of the propellant during the combustion process. As a result, the influence of aluminum particles on the combustion process, especially on the energy transfer on the surface, is more complicated than the assumptions in the model.

Finally, the model is established under ideal conditions, assuming that all the components react completely according to the given thermal decomposition process. In fact, both environmental factors, such as external temperature and pressure, and the

interaction between components have impact on the thermal decomposition. The thermal decomposition degree and the product cannot fully meet the assumptions.

To sum up, the improved free radical cracking model can provide qualitative guidance, to some extent, for the composition design of NEPE propellants. Error exists in comparison with the experimental data because of certain assumptions. Further improvement will be implemented in future studies based on the experimental result to make this model more accurate.

5 Conclusions

1. As the backpressure increases, the burning rate of NEPE propellants increases and the combustion flame becomes increasingly homogeneous and bright. An obvious diffusion flame structure appears for the aluminum-free NEPE propellant, while adding aluminum into the propellant causes more severe reactions in the reaction zone.

2. As oxidizers, the grain size of AP has more impact on the burning rate and the burning rate pressure exponent than the grain size of HMX. In comparison with the grain size of aluminum, both oxidizers' grain sizes have more impact on the burning rate but lighter impact on the burning rate pressure exponent.

3. For aluminum-free NEPE propellant, the reaction in the gas phase is dominant in the combustion. For aluminum-containing NEPE propellant, the reaction in the solid phase is dominant in the final stage since aluminum particles react both on the burning surface and in the gas phase reaction zone.

4. The addition of aluminum particles with smaller grain size makes the aluminum particle combustion zone closer to the burning surface and clearly increases the burning surface temperature. As a result, the heat feedback of the combustion of aluminum particles to the burning surface plays an essential role in the combustion process.

5. The improved free radical cracking model can be used to predict the burning rate of NEPE propellants and provide qualitative guidance, to some extent, for the composition design of NEPE propellants. However, its accuracy needs improvement.

Contributors

Xu-dong NA designed the research. Xiao-ting YAN and Xu-dong NA processed the corresponding data. Xiao-ting YAN wrote the first draft of the manuscript. Zhi-xun XIA and Li-ya HUANG helped to organize the manuscript. Xiao-ting YAN and Xu-dong NA revised and edited the final version.

Conflict of interest

Xiao-ting YAN, Zhi-xun XIA, Li-ya HUANG, and Xu-dong NA declare that they have no conflict of interest.

References

Benreuven M, 1980. Nitramine Monopropellant Deflagration and General Nonsteady Reacting Rocket Chamber Flows. PhD Thesis, Princeton University, Princeton, USA.

Benreuven M, Caveny LH, Vichnevetsky RJ, et al., 1977. Flame zone and sub-surface reaction model for deflagrating RDX. *Symposium (International) on Combustion*, 16(1):1223-1233. https://doi.org/10.1016/s0082-0784(77)80410-4

Davenas A, 1997. Solid Rocket Propulsion Technology. Zhang DX, translator. Astronautic Publishing House, Beijing, China (in Chinese).

Ermolin NE, Korobeinichev OP, Kuibida LV, et al., 1987. Study of the kinetics and mechanism of chemical reactions in hexogen flames. *Combustion, Explosion and Shock Waves*, 22(5):544-553. https://doi.org/10.1007/bf00755523

Fang YZ, Li SF, 2001. Experimental studies on effects of AP content and particle size in NEPE propellant. *Journal of Solid Rocket Technology*, 24(3):47-53 (in Chinese). https://doi.org/10.3969/j.issn.1006-2793.2001.03.011

Fry RS, DeLuca L, Frederick R, et al., 2002. Evaluation of Methods for Solid Propellant Burning Rate Measurements. Technical Report, NATO RTO Advisory Report, AVT Working Group 016.

Khichar M, Patidar L, Thynell ST, 2018. Improvement and validation of a detailed reaction mechanism for thermal decomposition of RDX in liquid phase. *Combustion and Flame*, 198:455-465. https://doi.org/10.1016/j.combustflame.2018.10.005

Khichar M, Patidar L, Thynell ST, 2019. Comparative analysis of vaporization and thermal decomposition of cyclotrimethylenetrinitramine (RDX). *Journal of Propulsion and Power*, 35(6):1098-1107. https://doi.org/10.2514/1.B37643

Li MM, Song HC, Wang Y, et al., 2008a. Modeling effects of aluminum content and particle size on NEPE combustion performance. *Chinese Journal of Energetic Materials*, 16(3):319-322 (in Chinese). https://doi.org/10.3969/j.issn.1006-9941.2008.03.020

Li MM, Song HC, Wang Y, et al., 2008b. Predicting effects of oxidizer content and particle size on NEPE combustion

characteristics. *Journal of Propulsion Technology*, 29(4): 502-507 (in Chinese).
https://doi.org/10.3321/j.issn:1001-4055.2008.04.022

Li MM, Wang Y, Guo XD, et al., 2009. Numerical simulation for burning rate of GAP high-energy propellant. *Journal of Solid Rocket Technology*, 32(5):535-538 (in Chinese).
https://doi.org/10.3969/j.issn.1006-2793.2009.05.016

Li SF, Fang C, 2002. "Linkage-mutualism" mechanism for interactions between AP and HMX. *Journal of Propulsion Technology*, 23(1):79-83 (in Chinese).
https://doi.org/10.3321/j.issn:1001-4055.2002.01.021

Li SF, Niu HL, Zhang GC, et al., 2002. Laser ignition of NEPE propellant. *Journal of Propulsion Technology*, 23(2): 172-175 (in Chinese).
https://doi.org/10.3321/j.issn:1001-4055.2002.02.022

Li XM, Liu YF, Yao WS, et al., 2001. Study on low burning rate NEPE propellant. *Chinese Journal of Explosives & Propellants*, 24(3):1-3 (in Chinese).
https://doi.org/10.3969/j.issn.1007-7812.2001.03.001

Liu YF, Yao WS, Li XM, et al., 2003. Combustion property of NEPE propellant. *Chinese Journal of Explosives & Propellants*, 26(4):30-32 (in Chinese).
https://doi.org/10.3969/j.issn.1007-7812.2003.04.010

Luo YJ, Liu JR, 2007. Research progress of high energy solid propellant. *Chinese Journal of Energetic Materials*, 15(4):407-410 (in Chinese).
https://doi.org/10.3969/j.issn.1006-9941.2007.04.029

Palopoli SF, Brill TB, 1991. Thermal decomposition of energetic materials 52. On the foam zone and surface chemistry of rapidly decomposing HMX. *Combustion and Flame*, 87(1):45-60.
https://doi.org/10.1016/0010-2180(91)90026-8

Pang AM, Wang BH, Tian DY, 2003. Combustion modeling of NEPE propellant. *Modern Defence Technology*, 31(2):29-32 (in Chinese).
https://doi.org/10.3969/j.issn.1009-086X.2003.02.006

Pang WQ, Fan XZ, Yi JH, et al., 2010. Thermal behavior and non-isothermal decomposition reaction kinetics of NEPE propellant with ammonium dinitramide. *Chinese Journal of Chemistry*, 28(5):687-692.
https://doi.org/10.1002/cjoc.201090132

Patidar L, Thynell ST, 2017. Quantum mechanics investigation of initial reaction pathways and early ring-opening reactions in thermal decomposition of liquid-phase RDX. *Combustion and Flame*, 178:7-20.
https://doi.org/10.1016/j.combustflame.2016.12.024

Patidar L, Khichar M, Thynell ST, 2018. Identification of initial decomposition reactions in liquid-phase HMX using quantum mechanics calculations. *Combustion and Flame*, 188:170-179.
https://doi.org/10.1016/j.combustflame.2017.09.042

Patidar L, Khichar M, Thynell ST, 2019. Modeling of HMX monopropellant combustion with detailed condensed-phase kinetics. AIAA Propulsion and Energy 2019 Forum.
https://doi.org/10.2514/6.2019-4210

Patidar L, Khichar M, Thynell ST, 2020. A comprehensive mechanism for liquid-phase decomposition of 1,3,5,7-tetranitro-1,3,5,7-tetrazoctane (HMX): thermolysis experiments and detailed kinetic modeling. *Combustion and Flame*, 212:67-78.
https://doi.org/10.1016/j.combustflame.2019.10.025

Peng PG, Liu DH, 1990. Ammonium perchlorate/nitramine propellant combustion simulation. *Journal of Propulsion Technology*, (4):63-70 (in Chinese).
https://doi.org/10.13675/j.cnki.tjjs.1990.04.011

Prasad K, Yetter RA, Smooke MD, 1997. An eigenvalue method for computing the burning rates of RDX propellants. *Combustion Science and Technology*, 124(1-6): 35-82.
https://doi.org/10.1080/00102209708935640

Prasad K, Yetter RA, Smooke MD, 1998. An eigenvalue method for computing the burning rates of HMX propellants. *Combustion and Flame*, 115(3):406-416.
https://doi.org/10.1016/s0010-2180(98)00009-1

Song HC, 1986. Gunpowder Combustion Model and Burning Rate Estimation Method. PhD Thesis, Nanjing University of Science and Technology, Nanjing, China (in Chinese).

Sun YL, Ren H, Jiao QJ, 2018. Comparison of thermal behaviors and decomposition kinetics of NEPE propellant before and after storage. *Journal of Thermal Analysis and Calorimetry*, 131(1):101-111.
https://doi.org/10.1007/s10973-017-6525-8

Wang F, Zhang XP, Hu RZ, et al., 2004. Study on combustion properties of nitrate ester plasticized polyether propellants at high pressure. *Journal of Propulsion Technology*, 25(5):469-472 (in Chinese).
https://doi.org/10.3321/j.issn:1001-4055.2004.05.019

Wang HM, Chen X, Zhao C, et al., 2015. Study on ignition and combustion characteristics of NEPE propellant under laser irradiation. *Journal of Propulsion Technology*, 36(8): 1262-1267 (in Chinese).
https://doi.org/10.13675/j.cnki.tjjs.2015.08.021

Wang SP, 2007. Combustion Mechanism and Burning Rate Estimation Program of Composite Solid Propellant. MS Thesis, Nanjing University of Science and Technology, Nanjing, China (in Chinese).

Xiang HS, Chen X, Zhou CS, et al., 2016. Effect of oxygen content in environment gas on the laser ignition process of NEPE propellant. *Chinese Journal of Explosives & Propellants*, 39(3):75-79 (in Chinese).
https://doi.org/10.14077/j.issn.1007-7812.2016.03.0015

Yang D, Zhao BC, Song HC, et al., 1997. Modeling for nitramine (RDX, HMX) propellant burning characteristics. *Journal of Nanjing University of Science and Technology*, 21(5):415-418 (in Chinese).
https://doi.org/10.14177/j.cnki.32-1397n.1997.05.009

Yetter RA, Dryer FL, Allen MT, et al., 1995. Development of gas-phase reaction mechanisms for nitramine combustion. *Journal of Propulsion and Power*, 11(4):683-697.
https://doi.org/10.2514/3.23894

Zhang XP, Dai ZL, 2007. Calculation for high-pressure

combustion properties of high-energy solid propellant based on GA-BP neural network. *Journal of Solid Rocket Technology*, 30(3):229-232 (in Chinese). https://doi.org/10.3969/j.issn.1006-2793.2007.03.012

Appendix A

Assuming that there are AP particles of various grain sizes in the propellant, the contents are a_{AP1}, a_{AP2}, …, $a_{\mathrm{AP}n}$, respectively, the grain sizes are d_{AP1}, d_{AP2}, …, $d_{\mathrm{AP}n}$, respectively, the total content of AP is a_{AP}, and the density of AP is ρ_{AP}.

The particle number of AP with single grain size in unit mass of propellant can be calculated as follows:

$$n_{\mathrm{AP}}=\frac{a_{\mathrm{AP}}}{\rho_{\mathrm{AP}}\left[\frac{4}{3}\pi\left(\frac{d_{\mathrm{AP}}}{2}\right)^3\right]}=\frac{6a_{\mathrm{AP}}}{\pi\rho_{\mathrm{AP}}d_{\mathrm{AP}}^3}. \tag{A1}$$

The total surface area of AP with single grain size in unit mass of propellant can be calculated as

$$S_{\mathrm{AP}}=n_{\mathrm{AP}}\cdot 4\pi\left(\frac{d_{\mathrm{AP}}}{2}\right)^2=\frac{6a_{\mathrm{AP}}}{\rho_{\mathrm{AP}}d_{\mathrm{AP}}}. \tag{A2}$$

Both the protruding and dent of AP particles will cause an increase of the burning area surface. S_0 is the unit cross-sectional area and S_0' is the corresponding burning surface area. The ratio between them is as follows:

$$\frac{S_0'}{S_0}=1+F_{11}\cdot\frac{a_{\mathrm{AP}}}{d_{\mathrm{AP}}}, \tag{A3}$$

where F_{11} is summarized from the experimental data.

The effect of AP content and the particle size on the combustion process can be attributed to the effect on the degree of cracking of the cleavable group, $\eta(p)$ function, and it directly depends on S_0'/S_0.

$$g_{\mathrm{AP}}=\left[\left(1+F_{11}\cdot\sum_{i=1}^{n}\frac{a_{\mathrm{AP}i}}{d_{\mathrm{AP}i}}\right)\cdot F_{12}\right]^{C_1}, \tag{A4}$$

where F_{12} and C_1 are to be determined.

The thickness of the equivalent reaction zone of $[NO_2]$ is L and can be obtained as

$$L=\int_{x_0}^{x_{\mathrm{d}}}\frac{\omega_j(x)}{\omega_j(x_0)}\mathrm{d}x=\sqrt{1+4\times a_{\mathrm{AP}}^2}, \tag{A5}$$

where the zone from x_0 to x_{d} is the inner flame reaction zone (Peng and Liu, 1990), $\omega_j(x)$ is the reaction rate of $[NO_2]$, and $\omega_j(x_0)$ is the mean reaction rate.

As a result,

$$f_{\mathrm{AP}}=\left(1+F_{11}\times\sum_{i=1}^{n}\frac{a_{\mathrm{AP}i}}{d_{\mathrm{AP}i}}\right)\sqrt{1+4a_{\mathrm{AP}}^2}. \tag{A6}$$

Through analyzing the experimental data, the values of g_{AP} and f_{AP} can be obtained:

$$g_{\mathrm{AP}}=\left(1+46.26\times\sum_{i=1}^{n}\frac{a_{\mathrm{AP}i}}{d_{\mathrm{AP}i}}\right)^{0.32}, \tag{A7}$$

$$f_{\mathrm{AP}}=\left(1+46.26\times\sum_{i=1}^{n}\frac{a_{\mathrm{AP}i}}{d_{\mathrm{AP}i}}\right)\sqrt{1+4\times\left(\sum_{i=1}^{n}a_{\mathrm{AP}i}\right)^2}. \tag{A8}$$

The effect mode and extent of HMX on the burning surface structure are different from that of AP. In this model, only the effect of a single layer of HMX particles on the burning surface is considered.

Assuming that there are various grain sizes of HMX in the propellant, the contents are respectively a_{HMX1}, a_{HMX2}, …, $a_{\mathrm{HMX}n}$, the grain sizes are respectively d_{HMX1}, d_{HMX2}, …, $d_{\mathrm{HMX}n}$, the total content of HMX is a_{HMX}, and the density is ρ_{HMX}.

The number of HMX particles with single grain size in unit volume is as follows:

$$n_{\mathrm{HMX}}=\frac{\rho_{\mathrm{P}}\cdot a_{\mathrm{HMX}}}{\rho_{\mathrm{HMX}}\cdot\frac{4}{3}\pi\cdot\left(\frac{d_{\mathrm{HMX}}}{2}\right)^3}. \tag{A9}$$

The number of HMX particles in a volume element with the cross-sectional area of 1 cm^2 is n_{HMX}'.

$$n_{\mathrm{HMX}}'=\left(n_{\mathrm{HMX}}\right)^{2/3}. \tag{A10}$$

The number of layers of HMX particles distributing in unit volume is n_{HMX}''.

$$n''_{\mathrm{HMX}}=\sqrt[3]{n_{\mathrm{HMX}}}. \tag{A11}$$

The effective surface area of HMX in the surface layer is S_{HMX}.

$$S_{\mathrm{HMX}}=n'_{\mathrm{HMX}}\cdot 4\pi\cdot\left(\frac{d_{\mathrm{HMX}}}{2}\right)^2\cdot\left(n''_{\mathrm{HMX}}\right)^{-1}. \tag{A12}$$

The relative increase of burning surface area is calculated as follows:

$$\left(\frac{S'}{S_0}\right)_2=1+F_{21}\cdot\left(\frac{\rho_{\mathrm{P}}}{\rho_{\mathrm{HMX}}}\right)^{\frac{1}{3}}\left(a_{\mathrm{HMX}}\right)^{\frac{1}{3}}\cdot d_{\mathrm{HMX}}, \tag{A13}$$

where F_{21} is to be determined.

The effects of HMX and AP on the decomposition products in the initial stage of propellant combustion are similar, and represented by g_{H}.

$$g_{\mathrm{H}}=\left[\left(\frac{S'}{S_0}\right)_2\right]^{C_2}, \tag{A14}$$

where C_2 is to be determined.

Ignoring the impact of HMX on the flame structure, f_{HMX} can be obtained:

$$f_{\mathrm{HMX}}=\prod_{i=1}^{n}\left[1+F_{22}\left(a_{\mathrm{HMX}i}\right)^{\frac{1}{3}}d_{\mathrm{HMX}i}\times10^{-4}\right], \tag{A15}$$

where F_{22} is an undetermined coefficient.

After analyzing the experimental results, f_{HMX} and g_{H} can be obtained as follows:

$$f_{\mathrm{HMX}}=\prod_{i=1}^{n}\left[1+11.73\left(a_{\mathrm{HMX}i}\right)^{\frac{1}{3}}d_{\mathrm{HMX}i}\times10^{-4}\right], \tag{A16}$$

$$g_{\mathrm{H}}=f_{\mathrm{HMX}}^{1.2}. \tag{A17}$$

Assuming that there are various grain sizes of aluminum in the propellant, the contents are respectively $a_{\mathrm{Al}1}$, $a_{\mathrm{Al}2}$, …, $a_{\mathrm{Al}n}$, the grain sizes (assumed to be spherical) are respectively $d_{\mathrm{Al}1}$, $d_{\mathrm{Al}2}$, …, $d_{\mathrm{Al}n}$, the total content of aluminum is a_{Al}, and the density is ρ_{Al}.

The number of aluminum particles with single grain size in unit mass is n_{Al}.

$$n_{\mathrm{Al}}=\frac{6a_{\mathrm{Al}}}{\pi\rho_{\mathrm{Al}}d_{\mathrm{Al}}^3}. \tag{A18}$$

The total surface area of aluminum particles with single grain size in unit mass is S_{Al}.

$$S_{\mathrm{Al}}=n_{\mathrm{Al}}\cdot 4\pi\left(\frac{d_{\mathrm{Al}}}{2}\right)^2=\frac{6a_{\mathrm{Al}}}{\rho_{\mathrm{Al}}d_{\mathrm{Al}}}. \tag{A19}$$

The ratio between S_0 and S_0' is calculated by

$$\left(\frac{S'_0}{S_0}\right)_4=1+F_{41}\cdot\frac{a_{\mathrm{Al}}}{d_{\mathrm{Al}}}, \tag{A20}$$

where F_{41} is to be determined.

The addition of aluminum particles affects not only the burning surface structure of NEPE propellants, but also the decomposition process on the burning surface at the initial stage of the reaction. This model approximates it to the effect on the $\eta(p)$ function, which could be described using g_{Al}:

$$g_{\mathrm{Al}}=\frac{1+F_{42}\cdot a_{\mathrm{Al}}}{d_{\mathrm{Al}}+C_{41}}, \tag{A21}$$

where F_{42} and C_{41} are to be determined.

The thickness of the equivalent reaction zone of $[NO_2]$ is calculated by

$$L=\int_{x_0}^{x_{\mathrm{d}}}\frac{\omega_j(x)}{\omega_j(x_0)}\mathrm{d}x=\sqrt{1+F_{43}\cdot a_{\mathrm{Al}}}\cdot\mathrm{e}^{-\left(0.1-a_{\mathrm{Al}}\right)^2\cdot C_{42}}, \tag{A22}$$

where F_{43} and C_{42} are to be determined.

As a result, the value of f_{Al} can be obtained as follows:

$$f_{\mathrm{Al}}=\left(1+F_{41}\frac{a_{\mathrm{Al}}}{d_{\mathrm{Al}}}\right)\sqrt{1+F_{43}a_{\mathrm{Al}}}\,\mathrm{e}^{-\left(0.1-a_{\mathrm{Al}}\right)^2C_{42}}. \tag{A23}$$

After analyzing the experimental results, the values of f_{Al} and g_{Al} can be obtained:

$$f_{\mathrm{Al}}=\left(1+0.015\times\frac{a_{\mathrm{Al}}}{d_{\mathrm{Al}}}\right)\sqrt{1+13a_{\mathrm{Al}}}\,\mathrm{e}^{-50\left(0.1-a_{\mathrm{Al}}\right)^2}, \tag{A24}$$

$$g_{\mathrm{Al}}=\frac{1+10a_{\mathrm{Al}}}{d_{\mathrm{Al}}+0.7}. \tag{A25}$$

中文概要

题　目：硝酸酯增塑聚醚（NEPE）推进剂燃烧的数值与试验研究

目　的：因 NEPE 推进剂具有独特的燃烧性能和燃烧机理，现有模型无法直接用于其燃烧相关研究。本文希望对现有模型进行改进，并基于自由基裂解模型建立一个计算 NEPE 推进剂燃速的模型，然后对 NEPE 推进剂燃烧进行观察和测量，研究其燃烧特性，以期为所建模型提供数据支持。

创新点：1. 基于自由基裂解模型，计算每种成分同时存在多种粒径分布的 NEPE 推进剂的燃速；2. 建立试验系统，观察 NEPE 推进剂燃烧火焰形态。

方　法：1. 通过理论推导，构建燃速与推进剂成分的粒径和含量以及燃烧室压强之间的关系，得到燃速计算公式（公式（1）–（10））；2. 利用建立的模型，计算四种不同粒径分布的 NEPE 推进剂在不同压强下的燃速，并与试验结果进行比较，验证模型的可行性（图 7）；3. 建立试验系统，测量 NEPE 推进剂的燃速和燃面温度，并观察其燃烧火焰（图 5 和 6），分析不同成分对燃烧的影响。

结　论：1. 基于自由基裂解模型建立的燃烧模型可用于预测 NEPE 推进剂的燃速；2. 铝颗粒的添加对 NEPE 推进剂的燃烧火焰形态和气相反应都有较大影响；3. 氧化剂（高氯酸铵和奥克托今）颗粒的粒径对燃速的影响比铝颗粒的粒径对燃速的影响大，但对燃速压强指数的影响相对较小。

关键词：NEPE 推进剂；燃烧；自由基裂解模型；试验研究